VIBRATIONAL STRUCTURE AND SYMMETRY IN $^{110-116}$Cd*

A. Leviatan

Racah Institute of Physics, The Hebrew University, Jerusalem 91904, Israel

J.E. García-Ramos

Department of Integrated Sciences
and Center for Advanced Studies in Physics
Mathematics and Computation, University of Huelva, 21071 Huelva, Spain

N. Gavrielov, P. Van Isacker

Grand Accélérateur National d'Ions Lourds, CEA/DRF-CNRS/IN2P3
Bvd Henri Becquerel, BP 55027, 14076 Caen, France

Received 12 November 2024, accepted 13 January 2025,
published online 10 April 2025

We show that a vibrational interpretation and good U(5) symmetry are maintained for the majority of low-lying normal states in ^{110,112,114,116}Cd isotopes, consistent with the empirical data. The observed deviations from this paradigm are properly treated by an interacting boson model Hamiltonian which breaks the U(5) symmetry in selected non-yrast states, while securing a weak mixing with coexisting SO(6)-like intruder states. The results demonstrate the relevance of the U(5) partial dynamical symmetry notion to this series of isotopes.

DOI:10.5506/APhysPolBSupp.18.2-A29

Even–even cadmium isotopes ($Z = 48$) near the neutron mid-shell have traditionally been considered textbook examples of spherical-vibrator motion and U(5) dynamical symmetry [1–3]. On the other hand, recent detailed studies using complementary spectroscopic methods have provided evidence for marked deviations from such a structural paradigm [4–7]. The low-lying spectra of these isotopes exhibit additional coexisting intruder states [8] associated with the promotion of two protons across the $Z = 50$ shell gap. Previous attempts to explain the observed discrepancies in E2 decays relied on strong mixing between vibrational and intruder states, and ultimately

* Presented at the 57$^{\text{th}}$ Zakopane Conference on Nuclear Physics, *Extremes of the Nuclear Landscape*, Zakopane, Poland, 25 August–1 September, 2024.

proved unsuccessful [5–7]. This paradoxical behavior has led to claims for the breakdown of vibrational motion in the isotopes $^{110-116}$Cd [5] and defines the so-called "Cd problem" [8].

Two approaches have been proposed to address these unexpected findings. The first abandons the traditional spherical-vibrational interpretation of the Cd isotopes, replacing it with multiple-shape coexistence of states in deformed bands, a view qualitatively supported by a beyond-mean-field calculation of ^{110,112}Cd with the Gogny D1S energy density functional [9, 10]. A second approach is based on the recognition that the reported deviations from a spherical-vibrator behavior show up in selected non-yrast states, while most states retain their vibrational character. In the terminology of symmetry, this implies that the symmetry in question is broken only in a subset of states, hence is partial [11]. In the present contribution, we follow the latter approach and show that the empirical data in $^{110-116}$Cd is compatible with a vibrational interpretation and U(5) partial symmetry for normal states, weakly coupled to deformed SO(6)-like intruder states [12, 13].

A convenient starting point for describing vibrations of spherical nuclei is the U(5) dynamical symmetry (DS) limit of the interacting boson model (IBM) [2], corresponding to the following chain of nested algebras:

$$\mathrm{U}(6) \supset \mathrm{U}(5) \supset \mathrm{SO}(5) \supset \mathrm{SO}(3)\,. \tag{1}$$

The associated DS basis states $|[N], n_d, \tau, n_\Delta, L\rangle$ are specified by quantum numbers which are the labels of irreducible representations of the algebras in the chain. Here, N is the total number of monopole (s) and quadrupole (d) bosons, n_d and τ are the d-boson number and seniority, respectively, L is the angular momentum, and n_Δ is a multiplicity label. The U(5)-DS Hamiltonian can be transcribed in the form

$$\begin{aligned}\hat{H}_{\rm DS} \;=\; & \rho_1 \hat{n}_d + \rho_2 \hat{n}_d\,(\hat{n}_d - 1) + \rho_3 \left[-\hat{C}_{\mathrm{SO}(5)} + \hat{n}_d(\hat{n}_d + 3)\right] \\ & + \rho_4 \left[\hat{C}_{\mathrm{SO}(3)} - 6\hat{n}_d\right]\,,\end{aligned} \tag{2}$$

where $\hat{C}_{\rm G}$ is a Casimir operator of the algebra G, and $\hat{n}_d = \sum_m d^\dagger_m d_m = \hat{C}_{\mathrm{U}(5)}$. $\hat{H}_{\rm DS}$ is completely solvable with eigenstates $|[N], n_d, \tau, n_\Delta, L\rangle$ and energies $E_{\rm DS} = \rho_1 n_d + \rho_2 n_d(n_d-1) + \rho_3[-\tau(\tau+3) + n_d(n_d+3)] + \rho_4[L(L+1) - 6n_d]$. The U(5)-DS spectrum resembles that of a spherical vibrator with states arranged in n_d-multiplets and strong ($n_d + 1 \to n_d$) E2 transitions with particular ratios, *e.g.*, $\frac{B(\mathrm{E2};\, n_d+1, L'=2n_d+2 \to n_d, L=2n_d)}{B(\mathrm{E2};\, n_d=1, L=2 \to n_d=0, L=0)} = (n_d+1)\frac{(N-n_d)}{N}$.

As a typical example, the empirical spectrum of ^{110}Cd, shown in Fig. 1, consists of both normal and intruder levels. At first sight, the normal states seem to follow the expected pattern of spherical-vibrator n_d-multiplets. As

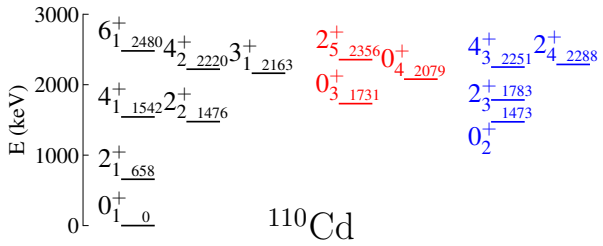

Fig. 1. (Color online) Experimental spectrum of ^{110}Cd in keV. Normal states are marked in black, or in red/light gray if their E2 decays deviate from those of a spherical vibrator and U(5) dynamical symmetry. Intruder states are marked in blue/gray. Data are taken from [14].

seen in Table 1, the measured E2 rates support this view for the majority of normal states, however, selected non-yrast states (shown in red/light gray in Fig. 1) reveal marked deviations from this behavior. Specifically, the 0^+_3 and 2^+_5 states in ^{110}Cd (denoted in Table 1 by 0^+_α and 2^+_α) which in the U(5)-DS classification are members of the $n_d = 2$ and $n_d = 3$ multiplets, respectively, have unusually small E2 rates for the transitions $0^+_\alpha \to 2^+_1$ and $2^+_\alpha \to 2^+_2$, and large rates for $0^+_\alpha \to 2^+_2$, at variance with the U(5)-DS predictions. Absolute B(E2) values for transitions from the 0^+_4 state are not known, but its branching ratio to the 2^+_2 state is small [6]. As shown in Table 1, the same unexpected decay patterns occur in all cadmium

Table 1. Comparison between experimental (EXP) and U(5)-DS predicted $B(\mathrm{E2}; L_\mathrm{i} \to L_\mathrm{f})$ values in Weisskopf units (W.u.) for normal states in $^{110-116}$Cd. The 0^+_α (2^+_α) state corresponds to the experimental $0^+_3, 0^+_3, 0^+_3, 0^+_2$ ($2^+_5, 2^+_4, 2^+_5, 2^+_4$) state for ^{A}Cd ($A = 110, 112, 114, 116$), respectively. In the U(5)-DS classification, $(0^+_1, 2^+_1, 2^+_2, 4^+_1, 6^+_1)$ are the class-A states with $n_d = 0, 1, 2, 2, 3$, and $(0^+_\alpha, 2^+_\alpha)$ are states with $n_d = (2, 3)$. Data are taken from [4–7, 14].

	^{110}Cd		^{112}Cd		^{114}Cd		^{116}Cd	
$L_\mathrm{i} \to L_\mathrm{f}$	EXP	U(5)	EXP	U(5)	EXP	U(5)	EXP	U(5)
$2^+_1 \to 0^+_1$	27.0(8)	27.0	30.31(19)	30.31	31.1(19)	31.1	33.5(12)	33.5
$4^+_1 \to 2^+_1$	42(9)	46	63(8)	53	62(4)	55	56(14)	59
$2^+_2 \to 2^+_1$	30(5)	46	39(7)	53	22(6)	55	25(10)	59
$2^+_2 \to 0^+_1$	0.68(14)	0	0.65(11)	0	0.48(6)	0	1.11(18)	0
$6^+_1 \to 4^+_1$	40(30)	58		68	119(15)	72	110^{+40}_{-80}	75
$0^+_\alpha \to 2^+_1$	< 7.9	46	0.0121(17)	53	0.0026(4)	55	0.79(22)	59
$0^+_\alpha \to 2^+_2$	< 1680	0	99(16)	0	127(16)	0		0
$2^+_\alpha \to 2^+_2$	$0.7^{+0.5}_{-0.6}$	11	$< 1.6^{+6}_{-4}$	13	2.5^{+16}_{-14}	14	2.0(6)	14
$2^+_\alpha \to 0^+_\alpha$	24.2(22)	27	25(7)	32	17(5)	34	35(10)	35

isotopes with mass number $A = 110$–116, and comprise the above-mentioned "Cd problem" [8]. We are thus confronted with a situation in which some states in the spectrum obey the predictions of U(5)-DS, while other states do not. These empirical findings signal a potential role for partial dynamical symmetry (PDS). In what follows, we show that an approach based on U(5) PDS provides a possible explanation for the Cd problem in these isotopes.

PDS-based approaches have been previously implemented in nuclear spectroscopy, in conjunction with the SU(3)-DS [15–18], and SO(6)-DS [19–22] chains of the IBM, relevant to axial and γ-soft deformed shapes, respectively. Here, we focus on U(5)-PDS associated with the chain (1). The construction of Hamiltonians with U(5)-PDS follows the general algorithm [11, 20] by adding to the U(5)-DS Hamiltonian of Eq. (2) terms which annihilate particular sets of U(5) basis states. This leads to

$$\hat{H}_{\rm PDS} \;=\; \hat{H}_{\rm DS} + r_0\, G_0^\dagger G_0 + e_0 \left(G_0^\dagger K_0 + K_0^\dagger G_0 \right) , \tag{3}$$

where $G_0^\dagger = [(d^\dagger d^\dagger)^{(2)} d^\dagger]^{(0)}$ and $K_0^\dagger = s^\dagger (d^\dagger d^\dagger)^{(0)}$. G_0 and K_0 annihilate the states $|[N], n_d = \tau, \tau, n_\Delta = 0, L\rangle$ with $L = \tau, \tau+1, \ldots, 2\tau-2, 2\tau$ which, therefore, remain solvable eigenstates of $\hat{H}_{\rm PDS}$ with good U(5) symmetry. Henceforth, we refer to this special subset of states as class-A states. While $\hat{H}_{\rm DS}$ (2) is diagonal in the U(5)-DS chain (1), the r_0 and e_0 terms are not. Accordingly, the remaining eigenstates of $\hat{H}_{\rm PDS}$ (3) are mixed with respect to U(5) and SO(5). The U(5)-DS is therefore preserved in a subset of eigenstates but is broken in others. By definition, $\hat{H}_{\rm PDS}$ exhibits U(5)-PDS.

The combined effect of normal and intruder states can be studied in the framework of the interacting boson model with configuration mixing (IBM-CM) [23, 24]. The latter is based on associating the different shell-model spaces of $0p$–$0h$, $2p$–$2h$, $4p$–$4h, \ldots$ particle–hole excitations with the corresponding boson spaces comprising of N, $N{+}2$, $N{+}4, \ldots$ bosons, which are subsequently mixed. For two configurations, the IBM-CM Hamiltonian can be cast in a matrix form

$$\hat{H} = \begin{bmatrix} \hat{H}_{\rm normal} & \hat{V}_{\rm mix} \\ \hat{V}_{\rm mix} & \hat{H}_{\rm intruder} \end{bmatrix} , \tag{4}$$

where $\hat{H}_{\rm normal}$ represents the normal configuration (N boson space), $\hat{H}_{\rm intruder}$ represents the intruder configuration ($N{+}2$ boson space), and $\hat{V}_{\rm mix}$ is a mixing term. This procedure has been used extensively for describing coexistence phenomena in nuclei [25–28].

In the present study, $\hat{H}_{\rm normal} = \hat{H}_{\rm PDS}$. $\hat{H}_{\rm intruder}$ contains quadrupole and rotational terms, $\hat{H}_{\rm intruder} = \kappa\hat{Q}_\chi \cdot \hat{Q}_\chi + \kappa'\hat{L}\cdot\hat{L} + \Delta$, where $\hat{Q}_\chi = d^\dagger s + s^\dagger\tilde{d} + \chi(d^\dagger\tilde{d})^{(2)}$ and Δ is an energy offset. The mixing term is $\hat{V}_{\rm mix} = \alpha\left[(s^\dagger)^2 + (d^\dagger d^\dagger)^{(0)}\right]$ + H.c., where H.c. means Hermitian conjugate. The eigenstates $|\Psi; L\rangle$ of $\hat{H}$ (4) involve a mixture of normal ($\Psi_{\rm n}$) and intruder ($\Psi_{\rm i}$) components in the $[N]$ and $[N+2]$ boson spaces

$$|\Psi; L\rangle = a\,|\Psi_{\rm n}; [N], L\rangle + b\,|\Psi_{\rm i}; [N+2], L\rangle\,, \qquad a^2 + b^2 = 1\,. \tag{5}$$

The IBM-CM model space consists of $[N] \oplus [N+2]$ boson spaces with $N = 7, 8, 9$, for $^{110-114}$Cd, respectively, and $N = 8$ for ^{116}Cd. The normal configuration corresponds in the shell model to having two-proton holes below the $Z = 50$ shell gap, and the intruder configuration corresponds to two-proton excitation from below to above this gap, creating $2p$–$4h$ states.

As shown in Fig. 2 and Table 2, the U(5)-PDS calculation of spectra and E2 rates provides a good description of the empirical data in $^{110-116}$Cd. It yields the same B(E2) values as those of U(5)-DS for the class-A states $(0_1^+, 2_1^+, 2_2^+, 4_1^+, 6_1^+)$, and reproduces correctly the E2 transitions involving the $(0_\alpha^+, 2_\alpha^+)$ states which deviate considerably from the U(5)-DS predictions. The origin of these features is revealed by examining the structure of the eigenfunctions of $\hat{H}$ (4), as discussed below.

Table 2. Comparison between experimental (EXP) and U(5)-PDS calculated $B(\mathrm{E2}; L_{\rm i} \to L_{\rm f})$ values in W.u. for normal levels in $^{110-116}$Cd. Notation of states as in Table 1.

	^{110}Cd		^{112}Cd		^{114}Cd		^{116}Cd	
$L_{\rm i} \to L_{\rm f}$	EXP	PDS	EXP	PDS	EXP	PDS	EXP	PDS
$2_1^+ \to 0_1^+$	27.0(8)	27.0	30.31(19)	30.31	31.1(19)	31.1	33.5(12)	33.5
$4_1^+ \to 2_1^+$	42(9)	46	63(8)	52	62(4)	55	56(14)	60
$2_2^+ \to 2_1^+$	30(5)	45	39(7)	51	22(6)	53	25(10)	59
$2_2^+ \to 0_1^+$	0.68(14)	0.0	0.65(11)	0.0	0.48(6)	0.0	1.11(18)	0.0
$6_1^+ \to 4_1^+$	40(30)	53		59	119(15)	70	110^{+40}_{-80}	79
$0_\alpha^+ \to 2_1^+$	< 7.9	0.08	0.0121(17)	0.0121	0.0026(4)	0.0026	0.79(22)	0.79
$0_\alpha^+ \to 2_2^+$	< 1680	43	99(16)	49	127(16)	61		60
$2_\alpha^+ \to 2_2^+$	$0.7^{+0.5}_{-0.6}$	0.124	$< 1.6^{+6}_{-4}$	0.08	2.5^{+16}_{-14}	0.005	2.0(6)	0.004
$2_\alpha^+ \to 0_\alpha^+$	24.2(22)	21	25(7)	28	17(5)	33	35(10)	33

Table 3 shows for states in the normal sector the percentage of the wave function within the normal configuration [the probability a^2 of $\Psi_{\rm n}$ in Eq. (5)], and the dominant U(5) n_d-component in $\Psi_{\rm n}$ and its probability (P_{n_d}). The class-A states $(0_1^+, 2_1^+, 2_2^+, 4_1^+, 6_1^+)$ are seen to be dominated by the normal component $\Psi_{\rm n}$ (large $a^2 \geq 90\%$) implying a weak mixing (small b^2) with the

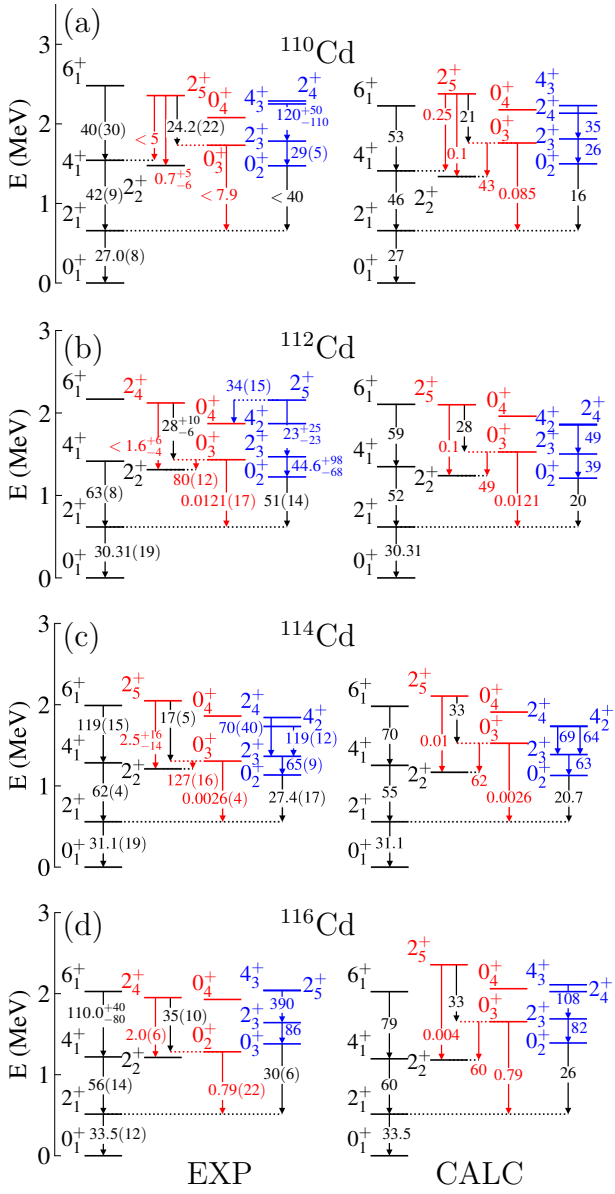

Fig. 2. Experimental (EXP) and calculated (CALC) energy levels in MeV and selected E2 transition rates in W.u. for (a) ^{110}Cd, (b) ^{112}Cd, (c) ^{114}Cd, (d) ^{116}Cd. The parameters of the PDS-CM Hamiltonian (4) and E2 transition operator employed in the calculation are given in [13].

Table 3. Configuration content and U(5) structure of the wavefunctions $|\Psi, L\rangle$, Eq. (5), of selected normal states, eigenstates of $\hat{H}$, Eq. (4). Shown are the probability (a^2) of the normal part $\Psi_{\rm n}$, the dominant n_d component in the U(5) decomposition of $\Psi_{\rm n}$, and its probability P_{n_d} (in %).

	^{110}Cd	^{112}Cd	^{114}Cd	^{116}Cd
L_k^+	a^2 (%) [(n_d) P_{n_d}]	a^2 (%) [(n_d) P_{n_d}]	a^2 (%) [(n_d) P_{n_d}]	a^2 (%) [(n_d) P_{n_d}]
0_1^+	98.23 [(0) 98.22]	97.94 [(0) 97.92]	97.98 [(0) 97.95]	98.27 [(0) 98.25]
2_1^+	96.38 [(1) 96.36]	95.10 [(1) 95.05]	95.28 [(1) 95.22]	96.84 [(1) 96.81]
4_1^+	90.73 [(2) 90.69]	83.19 [(2) 83.03]	83.05 [(2) 82.87]	92.95 [(2) 92.91]
2_2^+	89.81 [(2) 89.74]	81.62 [(2) 81.28]	78.77 [(2) 78.33]	91.31 [(2) 91.25]
6_1^+	71.18 [(3) 71.09]	42.92 [(3) 42.53]	39.46 [(3) 38.98]	79.34 [(3) 79.27]
0_α^+	70.75 [(3) 70.46]	71.13 [(3) 69.54]	71.55 [(3) 70.79]	74.34 [(3) 74.14]
2_α^+	68.34 [(4) 66.07]	65.89 [(4) 62.83]	40.78 [(4) 40.13]	55.68 [(4) 54.73]

intruder states. The 6_1^+ state experiences a larger mixing consistent with its enhanced decay to the lowest 4^+ intruder state [7, 14]. The normal–intruder mixing increases with L for a given isotope, and increases towards mid-shell (^{114}Cd) correlated with the decrease in energy of intruder states. The class-A states possess good U(5) quantum numbers to a good approximation. The U(5) decomposition of their $\Psi_{\rm n}$ part discloses a single n_d component with probability $P_{n_d} \geq 90\%$ and n_d-values similar to the U(5)-DS assignments. Such a high n_d-purity is a characteristic feature of spherical type of states and U(5) dynamical symmetry.

The non-yrast 0_α^+ and 2_α^+ states are more susceptible to the normal–intruder mixing but still retain the dominance of the normal component $\Psi_{\rm n}$ ($a^2 \sim 70\%$) and show a similar variation of the normal–intruder mixing, as a function of neutron number along the cadmium chain. However, in contrast to class-A states, their U(5) structure changes dramatically. Specifically, as is evident from Table 3, the $\Psi_{\rm n}$ parts of the 0_α^+ and 2_α^+ states, which in the U(5)-DS classification have $n_d = 2$ and $n_d = 3$, have now dominant components with $n_d = 3$ and $n_d = 4$, respectively. The change $n_d \mapsto (n_d+1)$ ensures weak ($\Delta n_d = 2$) transitions from these states to class-A states, but secures strong $2_\alpha^+ \to 0_\alpha^+$ ($\Delta n_d = 1$) transitions, in agreement with the data shown in Table 2.

While the class-A and $(0_\alpha^+, 2_\alpha^+)$ states are predominantly spherical, the intruder states are members of a single deformed band exhibiting a γ-soft spectrum, with characteristic 0^+, 2^+, $(4^+, 2^+)$ grouping of levels, shown in Fig. 2. Such a pattern resembles that encountered in the SO(6)-DS limit of the IBM associated with the chain U(6) $\supset$ SO(6) $\supset$ SO(5) $\supset$ SO(3) and related basis states $|[N], \sigma, \tau, n_\Delta, L\rangle$. Table 4 shows for states in the intruder

Table 4. Configuration content and SO(6) structure of the wavefunctions $|\Psi, L\rangle$, Eq. (5), of selected intruder states, eigenstates of $\hat{H}$, Eq. (4). Shown are the probability (b^2) of the intruder part $\Psi_{\rm i}$, the dominant σ component in the SO(6) decomposition of $\Psi_{\rm i}$, and its probability P_σ (in %). The $0^+_{1;i}$, $2^+_{1,i}$, $2^+_{2;i}$ and $4^+_{1;i}$ states, correspond to the experimental $(0^+_2, 0^+_2, 0^+_2, 0^+_3)$, $(2^+_3, 2^+_3, 2^+_3, 2^+_3)$, $(2^+_4, 2^+_5, 2^+_4, 2^+_5)$, and $(4^+_3, 4^+_2, 4^+_2, 4^+_3)$ states for ^{A}Cd ($A = 110, 112, 114, 116$), respectively.

	^{110}Cd	^{112}Cd	^{114}Cd	^{116}Cd
$L^+_{k;i}$	b^2 (%) [(σ) P_σ]	b^2 (%) [(σ) P_σ]	b^2 (%) [(σ) P_σ]	b^2 (%) [(σ) P_σ]
$0^+_{1;i}$	67.28 [(9) 67.11]	75.45 [(10) 75.29]	86.44 [(11) 86.33]	71.52 [(10) 71.30]
$2^+_{1;i}$	91.83 [(9) 91.60]	87.77 [(10) 87.44]	87.37 [(11) 87.00]	92.91 [(10) 92.75]
$2^+_{2,i}$	90.53 [(9) 90.15]	85.07 [(10) 84.49]	85.57 [(11) 84.99]	92.29 [(10) 91.99]
$4^+_{1;i}$	76.69 [(9) 76.13]	74.01 [(10) 73.43]	78.59 [(11) 77.98]	75.47 [(10) 74.83]

sector the percentage of the wave function within the intruder configuration [the probability b^2 of $\Psi_{\rm i}$ in Eq. (5)], the dominant SO(6) σ component in $\Psi_{\rm i}$, and its probability (P_σ). The intruder states are seen to have small mixing with the normal states (large b^2). Their wave functions exhibit a broad n_d-distribution, as expected for deformed type of states, and a pronounced SO(6) quantum number, $\sigma = N + 2$, albeit with a slight breaking of SO(5) symmetry induced by the quadrupole term in $\hat{H}_{\rm intruder}$, Eq. (4).

In summary, the results reported in the present contribution suggest that the vibrational interpretation and related U(5) dynamical symmetry description of $^{110-116}$Cd can be salvaged by considering a Hamiltonian with U(5)-PDS acting in the normal sector of spherical states with weak coupling to the intruder sector of SO(6)-like deformed states.

REFERENCES

[1] A. Bohr, B.R. Mottelson, «Nuclear Structure. II Nuclear Deformations», *Benjamin*, New York 1975.

[2] F. Iachello, A. Arima, «The Interacting Boson Model», *Cambridge University Press*, Cambridge 1987.

[3] R.F. Casten, «Nuclear Structure from a Simple Perspective», *Oxford University Press*, Oxford 2000.

[4] P.E. Garrett *et al.*, *Phys. Rev. C* **75**, 054310 (2007).

[5] P.E. Garrett, K.L. Green, J.L. Wood, *Phys. Rev. C* **78**, 044307 (2008).

[6] P.E. Garrett, J.L. Wood, *J. Phys. G: Nucl. Part. Phys.* **37**, 064028 (2010); *ibid.* **37**, 069701 (2010).

[7] P.E. Garrett *et al.*, *Phys. Rev. C* **86**, 044304 (2012).

[8] K. Heyde, J.L. Wood, *Rev. Mod. Phys.* **83**, 1467 (2011).
[9] P.E. Garrett *et al.*, *Phys. Rev. Lett.* **123**, 142502 (2019).
[10] P.E. Garrett *et al.*, *Phys. Rev. C* **101**, 044302 (2020).
[11] A. Leviatan, *Prog. Part. Nucl. Phys.* **66**, 93 (2011).
[12] A. Leviatan, N. Gavrielov, J.E. García-Ramos, P. Van Isacker, *Phys. Rev. C* **98**, 031302(R) (2018).
[13] N. Gavrielov, J.E. García-Ramos, P. Van Isacker, A. Leviatan, *Phys. Rev. C* **108**, L031305 (2023).
[14] Evaluated Nuclear Structure Data File (ENSDF), `https://www.nndc.bnl.gov/ensdf/`
[15] A. Leviatan, *Phys. Rev. Lett.* **77**, 818 (1996).
[16] A. Leviatan, J.E. García-Ramos, P. Van Isacker, *Phys. Rev. C* **87**, 021302(R) (2013).
[17] A. Leviatan, D. Shapira, *Phys. Rev. C* **93**, 051302(R) (2016).
[18] A. Leviatan, *Eur. Phys. J. Spec. Top.* **229**, 2405 (2020).
[19] A. Leviatan, P. Van Isacker, *Phys. Rev. Lett.* **89**, 222501 (2002).
[20] J.E. García-Ramos, A. Leviatan, P. Van Isacker, *Phys. Rev. Lett.* **102**, 112502 (2009).
[21] C. Kremer *et al.*, *Phys. Rev. C* **89**, 041302(R) (2014).
[22] P. Van Isacker, J. Jolie, T. Thomas, A. Leviatan, *Phys. Rev. C* **92**, 011301(R) (2015).
[23] P.D. Duval, B.R. Barrett, *Phys. Lett. B* **100**, 223 (1981).
[24] P.D. Duval, B.R. Barrett, *Nucl. Phys. A* **376**, 213 (1982).
[25] M. Sambataro, G. Molnar, *Nucl. Phys. A* **376**, 201 (1982).
[26] J.E. García-Ramos, K. Heyde, *Phys. Rev. C* **92**, 034309 (2015).
[27] K. Nomura, J. Jolie, *Phys. Rev. C* **98**, 024303 (2018).
[28] N. Gavrielov, A. Leviatan, F. Iachello, *Phys. Rev. C* **105**, 014305 (2022).